

# Phospholipid membranes affect tertiary structure of the soluble cytochrome *b*<sub>5</sub> heme-binding domain

Liana V. Basova <sup>a,1</sup>, Elisaveta I. Tiktopulo <sup>a</sup>, Victor P. Kutysenko <sup>b</sup>,  
A. Grant Mauk <sup>c</sup>, Valentina E. Bychkova <sup>a,\*</sup>

<sup>a</sup> Institute of Protein Research, Russian Academy of Sciences, Pushchino, Moscow Region, 142290 Russia

<sup>b</sup> Institute for Theoretical and Experimental Biophysics, Russian Academy of Sciences, Pushchino, Moscow Region, 142290 Russia

<sup>c</sup> Department of Biochemistry and Molecular Biology and the Centre for Blood Research,  
University of British Columbia, Vancouver, British Columbia, Canada V6T 1Z3

Received 24 August 2007; received in revised form 21 December 2007; accepted 28 December 2007

Available online 17 January 2008

## Abstract

The influence of charged phospholipid membranes on the conformational state of the water-soluble fragment of cytochrome *b*<sub>5</sub> has been investigated by a variety of techniques at neutral pH. The results of this work provide the first evidence that aqueous solutions with high phospholipid/protein molar ratios (pH 7.2) induce the cytochrome to undergo a structural transition from the native conformation to an intermediate state with molten-globule like properties that occur in the presence of an artificial membrane surface and that leads to binding of the protein to the membrane. At other phospholipid/protein ratios, equilibrium was observed between cytochrome free in solution and cytochrome bound to the surface of vesicles. Inhibition of protein binding to the vesicles with increasing ionic strength indicated for the most part an electrostatic contribution to the stability of cytochrome *b*<sub>5</sub>–vesicle interactions at pH 7.2. The possible physiological role of membrane-induced conformational change in the structure of cytochrome *b*<sub>5</sub> upon the interaction with its redox partners is discussed.

© 2008 Elsevier B.V. All rights reserved.

**Keywords:** Cytochrome *b*<sub>5</sub> water-soluble fragment; Artificial membranes; Protein denaturation; Intermediate state

## 1. Introduction

The involvement of non-native intermediate protein states such as the molten globule [1] in some cellular processes is well known. Processes in which molten-globule states are believed to participate include translocation of proteins across membranes, protein-protein interactions, and protein degradation. Assuming that cytoplasmic proteins occur predominantly in the native state, the question arises concerning the mechanism by which the corresponding molten-globule states are formed. In cells, a variety of situations occur in which proteins are exposed to a denaturing environment as may be presented, for example, by low pH (as

occurs in some organelles), heat shock or various membrane structures (especially negatively charged membranes) [2]. The physical basis for the denaturing action of membrane surfaces is a local, moderate decrease in pH and, probably more important, local, moderate decrease of dielectric constant that will enhance electrostatic interactions near a membrane surface. A simple approach to modeling these conditions has been proposed in which proteins are exposed to water–alcohol mixtures at moderately low pH [3]. This strategy was proposed because only alcohols denature proteins in proportion to the decrease in dielectric constant of water–alcohol mixtures [4,5].

To evaluate this hypothesis, several proteins that function near a membrane surface and that vary in their net electrostatic charge have been studied to assess the structural consequences of moderate changes in both pH and dielectric constant, and this behavior has been compared to the behavior of these proteins near phospholipid membranes. Proteins used in these studies include (a) the nearly neutral retinol-binding protein

\* Corresponding author. Tel./fax: +7 495 6327871.

E-mail addresses: [bychkova@vega.protnet.ru](mailto:bychkova@vega.protnet.ru), [vbychkova@mail.ru](mailto:vbychkova@mail.ru) (V.E. Bychkova).

<sup>1</sup> Present address: Department of Biochemistry, Medical College of Wisconsin, Milwaukee, WI USA.

[6,7] that transports vitamin A, (b) positively charged cytochrome *c* [3,8–11] that functions in the intermembrane space of mitochondria, and (c) neutral apo- [12,13] and holomyoglobins ([14,15] and Basova et al., manuscript in preparation) that are involved in dioxygen transport. Recently, similar studies have been initiated with the negatively charged, water-soluble heme-binding domain of cytochrome *b*<sub>5</sub> (wsCyt *b*<sub>5</sub>) that functions as an electron donor for redox enzymes located on the surface of the endoplasmic reticulum in which the structural consequences of exposure of the wsCyt *b*<sub>5</sub> to water–methanol mixtures [16] and water–isopropanol mixtures (unpublished data) have been evaluated.

The current report presents the experimental characterization of the water-soluble fragment of cyt *b*<sub>5</sub> in the presence and absence of phospholipid vesicles. The results provide the first evidence that proximity to a negatively charged membrane surface can destabilize the structure of wsCyt *b*<sub>5</sub> at neutral pH and facilitate its transition into a more flexible conformational state with molten globule-like properties. This more flexible state of the protein is the form that interacts with the artificial membrane surface. Although natural membrane surfaces are more complex than those of phospholipid vesicles, results obtained with them should reflect the changes in protein tertiary structure to be expected for proteins that function near a membrane surface.

WsCyt *b*<sub>5</sub> is similar to myoglobin in that heme binds non-covalently to the apo-protein, but it differs in that the net charge on the cytochrome is large and negative rather than almost neutral. Cyt *b*<sub>5</sub> is a small, heme-containing, two-domain membrane protein (16 kDa) [17] comprised of a hydrophilic heme-binding domain and a hydrophobic C-terminal membrane-binding domain that anchors the protein to the endoplasmic reticulum. The hydrophilic heme-binding domain is solely responsible for the electron-transfer functions of the protein. The heme-binding domain of the microsomal cytochrome can be isolated as a water-soluble protein (~10 kDa) following tryptic hydrolysis of the membrane-binding form of the cytochrome [18,19]. The structure and electron-transfer properties of this soluble domain have been studied extensively [20–29]. The negatively charged residues at the surface of cytochrome *b*<sub>5</sub> near the partially-exposed heme edge are well conserved among various species of microsomal cytochrome *b*<sub>5</sub>, and these residues participate [30] in the interactions with other electron-transfer proteins and enzymes to which the cytochrome transfers electrons [31], which are mainly membrane proteins.

As indicated above, binding of full-length cyt *b*<sub>5</sub> to membranes is mediated by a hydrophobic C-terminal sequence that is separated from the hydrophilic, heme-binding domain by 10 amino acid residues so that the heme-binding domain must reside in proximity to the membrane surface [17,32,33]. In the erythrocyte, however, most of the cyt *b*<sub>5</sub> is not membrane bound and is found in the cytoplasm. This form of the protein is reduced by methemoglobin reductase (which is actually a cyt *b*<sub>5</sub> reductase [34,35]) and reduced erythrocytic cyt *b*<sub>5</sub> then reduces methemoglobin to deoxyhemoglobin to return the oxidized protein to the form that is required for dioxygen transport [36]. In addition to the microsomal cytochrome, a mitochondrial form of cyt *b*<sub>5</sub> has been identified [37,38]. Though this cytochrome is

very similar to the microsomal cytochrome, the two proteins exhibit slightly different electron-transfer properties [39] and different heme-binding orientation disorder equilibria [40,41]. All these forms of cyt *b*<sub>5</sub> participate in several reactions [31, 36,42–44], many of which occur at or near membrane surfaces and all of which involve protein-protein interactions.

Thus, we propose that the tertiary structure of the wsCyt *b*<sub>5</sub> may be affected by the presence of membrane surfaces and that these structural changes could influence the interaction of the cytochrome domain with its partners, e.g., cyt *b*<sub>5</sub>-reductase [45], cyt P450 [46,47]. It should be emphasized that previous studies indicated that the water-soluble fragment of cyt *b*<sub>5</sub> does not bind to neutral membranes composed from DOPC [20]. Thus, the current study considers the possible interaction of this protein under conditions, where wsCyt *b*<sub>5</sub> is in the native state (at pH 7.2 and 5.5), with negatively charged phospholipid membranes as models of the membrane surfaces which might facilitate conformational changes in protein structure and the interactions of cytoplasmic domains of redox partners. Previously, we investigated the effect of pH-induced denaturation of wsCyt *b*<sub>5</sub> [48] to evaluate the possible structural consequences of the suggestion that the pH can decrease at least 2 pH units near membrane surfaces [49]. If this proposal is correct, the native cytochrome structure should dominate at pH 7.2 in the presence of a phospholipid membrane surface, but at pH 5.5 the model membrane should induce the protein to form an intermediate molten globule-like state similar to that observed in aqueous solution at pH 3.0 [48]. The side-chain packing and protein tertiary structure (near-UV CD spectra), thermal stability (differential scanning calorimetry), integrity of the heme-binding pocket (Soret absorbance), the integrity of the environment of the Trp side chain (fluorescence emission spectrum), and secondary structure (far-UV CD spectra) were monitored by the methods indicated to assess the structural response of the cytochrome to exposure to phospholipid membranes.

## 2. Materials and methods

### 2.1. Protein preparation

The recombinant, water-soluble heme-binding domain of cyt *b*<sub>5</sub> was expressed in *Escherichia coli* and purified by ion exchange [50] and gel-filtration (Ultrogel AcA 54 (IBF BioTechnics, France) chromatography. Cytochrome-containing fractions with an absorbance ratio  $A_{412}/A_{280} \geq 5.0$  were collected, and protein purity ( $\geq 98\%$ ) was verified by gel electrophoresis under denaturing conditions. The concentration of wsCyt *b*<sub>5</sub> solutions was determined from the intensity of the Soret absorbance ( $A_{412} = 117,000 \text{ M}^{-1} \text{ cm}^{-1}$  [17], or  $A_{412} = 10.8$  for 1 mg/ml/cm) with a Shimadzu UV-1601 spectrophotometer (Japan). The completely unfolded state (U) of wsCyt *b*<sub>5</sub> was obtained in 6.0 M guanidinium chloride (GdmCl).

### 2.2. Small unilamellar vesicles (SUV) preparation

Small unilamellar vesicles (SUV) used as model membrane structures were prepared as described previously [51,52]. SUV-like parts of cellular membranes have the most active surface (similar to the tortuous portions of the mitochondrial membrane) and can impact protein structures, if any. Two types of negatively charged phospholipids were used: 1-Palmitoyl-2-Oleoyl-sn-Glycero-3-Phosphatidylglycerol (POPG; 770.99 Da) and 1,2-Dipalmitoyl-sn-Glycero-3-Phosphatidylglycerol (DPPG; 744.96 Da), and one neutral-1,2-dipalmitoyl-sn-

Glycero-3-Phosphatidylcholine (DPPC; 734.05 Da), all of which were obtained from Avanti Polar Lipids (Alabaster, AL, USA). Phosphatidylglycerol derivatives were chosen for their ability to form perfect bilayer structures, and most experiments were performed with POPG vesicles. DPPG vesicles were used only in microcalorimetric studies to visualize changes in vesicles simultaneously with protein structure melting. Phospholipids were dissolved in chloroform, which was evaporated under nitrogen and dried overnight under vacuum. The resulting film was hydrated in an aqueous buffer (0.01 M sodium phosphate, pH 7.2 and pH 5.5) by sonication at 22 kHz for 10 min with an UZDN-2T sonicator (SEMI, Ukraine) [52]. This procedure produced small unilamellar vesicles (SUV) with a diameter in the range of 300–500 Å as indicated by both dynamic light scattering and macroscopic diffusion (data not shown).

### 2.3. Preparation of wsCyt $b_5$ -vesicle mixtures

WsCyt  $b_5$  solution was added to phospholipid vesicle suspensions to obtain mixtures with a molar ratio of phospholipids to protein that varied from 50:1 to 500:1 at pH 7.2 and from 25:1 to 200:1 at pH 5.5. Samples at high ionic strength (150 mM NaCl) were prepared by addition of sodium chloride solution (1.0 M) to premixtures of wsCyt  $b_5$  and vesicles (after protein-vesicle complex formation) at pH 7.2. To avoid any contribution of kinetics in interaction of protein molecules and vesicles, a mixture of phospholipids vesicle suspension and wsCyt  $b_5$  solution was kept overnight before measurements.

### 2.4. Differential scanning calorimetry

The thermal stability of wsCyt  $b_5$  (0.8–1.0 mg/ml) in the presence and absence of phospholipid vesicles was evaluated and control measurements for the vesicles in buffer were obtained with a SCAL-1 differential scanning microcalorimeter (Scal Co., Pushchino, Russia) at a heating rate of 1 °C/min in a 0.3-ml glass cell. The phospholipids concentration was adjusted to achieve the desired phospholipid/protein molar ratio. The resulting thermodynamic data were analyzed as described previously [53].

### 2.5. Spectroscopy

The circular dichroism (CD) spectra of wsCyt  $b_5$  in the presence and absence of phospholipid vesicles were recorded with a Jasco Model J-600 spectropolarimeter (Japan). Spectra in the far-UV region were obtained with an optical path length of 0.2 mm, and spectra in the near-UV region were obtained with an optical path length of 1 cm. Tryptophan fluorescence emission spectra (300–500 nm) of wsCyt  $b_5$  (0.1 mg/ml) in the presence and absence of phospholipid vesicles were recorded with a Shimadzu Model RF-5301 PC spectrofluorimeter (1 cm path length) using an excitation wavelength of 293 nm.  $^1\text{H-NMR}$  spectra of wsCyt  $b_5$  (2.5, 5 mg/ml) were obtained in the presence and absence of phospholipid membranes with an Avance 600 spectrometer at 600 MHz (Bruker, Germany). The spectral width was 8000 Hz, 90°-pulse – 10  $\mu\text{s}$ , number scans – 64–128.

### 2.6. Size exclusion chromatography

FPLC was performed with a Superdex 75 HR 10/30 column (Amersham Pharmacia Biotech, Sweden) that was equilibrated and developed (0.4 ml/min) with 10 mM sodium phosphate buffer (pH 7.2 and pH 5.5) supplemented with 150 mM NaCl. The column was calibrated with a standard protein chromatography calibration kit (Combithek, Germany). Elution of protein was monitored by UV absorption at 280 nm, and elution of phospholipid vesicles was monitored at 226 nm.

## 3. Results

### 3.1. Probing the rigid tertiary structure

To study the changes in overall protein tertiary structure, thermal stability (melting) and near-UV CD spectra are the most

informative initial approaches. For further insight, spectroscopic methods (e.g., fluorescence emission) are used to check changes in the immediate environment of tryptophans or prosthetic groups in different parts of the protein molecule.

#### 3.1.1. Microcalorimetry

In the presence of vesicles formed from POPG at low ionic strength, pH 7.2 and a phospholipid to protein molar ratio (L/P) of 50:1 (Fig. 1, curve 2), the heat absorption peak of wsCyt  $b_5$  is reduced relative to that of the native protein (curve 1), but the melting temperature remains nearly unchanged. This decrease in enthalpy may be explained by a decrease in the concentration of unbound protein in solution. At L/P of 100:1 (Fig. 1, curve 3) and greater, no heat absorption peak is observed at pH 7.2, indicating that the tertiary structure of the protein is disrupted under these conditions.

To detect possible electrostatic interaction of wsCyt  $b_5$  with vesicles, we studied the thermal melting of the protein with added salt. Experimental data obtained for the native protein in the absence and presence of vesicles at L/P of 50:1 and 150 mM NaCl are shown in Fig. 1 (curves 4 and 5). As can be seen, the addition of 150 mM sodium chloride to wsCyt  $b_5$  solution has little or no influence on the melting temperature but does increase slightly the calorimetric enthalpy for the native protein. For the 50:1 molar ratio L/P addition of 150 mM NaCl after complex formation results in an increase in peak intensity (Fig. 1, curves 2 and 5). This observation can be explained by the release of wsCyt  $b_5$  molecules previously bound to vesicles and restoration of the (unbound) form that melts at this temperature. The restoration of this thermally-responsive form of the protein by increasing ionic

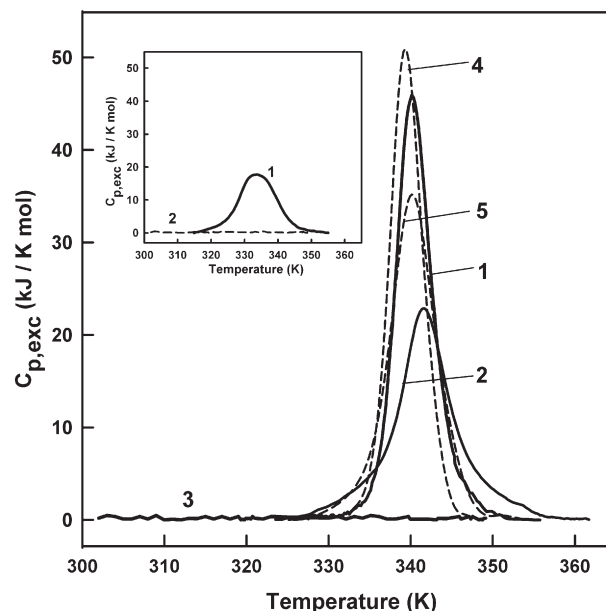


Fig. 1. Temperature dependence of the excess partial heat capacity  $C_{p,exc}$  for wsCyt  $b_5$ : at pH 7.2 at low (10 mM phosphate buffer, curves 1, 2, 3) and high (150 mM NaCl, curves 4, 5) ionic strength in the absence of phospholipid vesicles (curves 1, 4) and in the presence of vesicles at POPG/wsCyt  $b_5$  50:1 (curve 2, 5) and 100:1 (curve 3); (Inset) at pH 5.5 without vesicles (curve 1) and at POPG/wsCyt  $b_5$  25:1 at pH 5.5 (curve 2). Protein concentration was 1.0 mg/ml.

strength is confirmed by the Trp fluorescence and the Soret band absorbance observed under these conditions (data not shown).

A much different picture is observed at low ionic strength at pH 5.5 (Fig. 1, inset), where even at a 25:1 molar ratio (curve 2), the heat absorption peak is absent. As can be seen, both the shape and intensity of the heat absorption peak are altered under these conditions. Thus, at pH 5.5 (Fig. 1, inset) the rigid native protein structure is perturbed even in the absence of vesicles (curve 1) and more greatly changed in the presence of negatively charged vesicles than at pH 7.2 (see Fig. 1). It should be emphasized that the change in the heat absorption peak at pH 5.5 in comparison to that at pH 7.2 reflects pH-dependent destabilization of the thermal stability of the wsCyt  $b_5$  tertiary structure, but the protein remains in the native state (see the near-UV CD spectrum at this pH, below).

The effect of phospholipids is more pronounced in the presence of DPPG vesicles at a 50:1 L/P and pH 7.2 (Fig. 2 a). The  $C_{p,exc}$  value, calculated on the basis of phospholipid concentration, is in the range of that for pure phospholipid vesicles, but the heat absorption peak for the protein is drastically reduced ( $C_{p,exc}$  value for wsCyt  $b_5$ , calculated on the basis of total protein concentration, is very low) though still present. The second heating at pH 7.2 does not change the position of the heat absorption peak for vesicles in the presence (Fig. 2 a) or in the absence (Fig. 2 b) of the protein, but the heat absorption peak for the protein is absent from the second heating. At L/P of 100:1 and pH 7.2, the melting of vesicles coincides with that at the 50:1 ratio, but no absorption peak is observed for the protein (data not shown). On decreasing pH to 5.5, the protein-vesicle interaction is more readily apparent as seen by comparing the

heat absorption peaks of vesicles in the presence (Fig. 2 c) and absence (Fig. 2 d) of wsCyt  $b_5$  at L/P of 25:1. In the presence of the protein, a significant difference is observed between the first and second heating of the sample while for vesicle preparations lacking protein, this difference is nearly absent (Fig. 2 d). This result indicates that at pH 5.5 the protein-vesicle interaction is more readily evident. Such behavior may be explained by disturbance in the packing of phospholipids in the vesicle bilayer. Increase of the heat absorbance peak after the second heating may indicate the occurrence of hydrogen bonding between protein molecules and the vesicle surface at pH 5.5, and a change in the shape and position of the peak (Fig. 2 c) may reflect even hydrophobic interactions, leading to more cooperative protein-vesicle system. POPG and DPPG both exert a denaturing effect on the wsCyt  $b_5$  structure, but the DPPG effect is slightly stronger presumably because it presents a better ordered negatively charged membrane surface than does POPG. Such a difference in membrane lipid organization is expected because DPPG contains saturated fatty acids that are capable of more efficient packing while POPG contains unsaturated fatty acid tails that are less flexible and pack in more irregular arrays. In general, however, vesicles formed by both lipids exhibit a similar denaturing influence on protein structure, but using POPG permits characterization of any interactions at one and the same liquid-crystalline phase of phospholipids bilayer at room temperature and higher.

Taken together, the changes in the shape and intensity of the heat absorption peak observed above support the conclusion that the rigid native protein structure is destabilized in the presence of negatively charged vesicles. At pH 7.2, virtually no change in

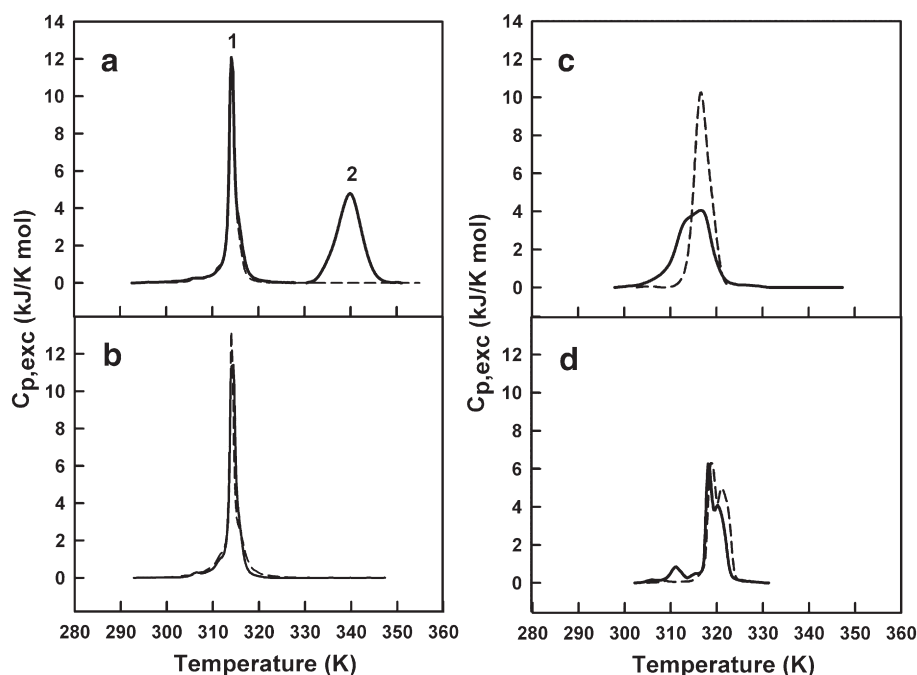


Fig. 2. Excess partial heat capacity,  $C_{p,exc}$  as a function of temperature for DPPG vesicles in the presence of wsCyt  $b_5$  at pH 7.2 at DPPG/wsCyt  $b_5$  molar ratios of (a) 50:1 (1-DPPG peak, 2-wsCyt  $b_5$  peak) and (b) pure DPPG vesicles. At a molar ratio 50:1, the  $C_{p,exc}$  peak in the range of 340 K range was calculated for a protein concentration 0.8 mg/ml and the  $C_{p,exc}$  peak in the range of 315 K was calculated for the appropriate DPPG concentration. Similar measurements were obtained for DPPG vesicles at pH 5.5 (c) in the presence of wsCyt  $b_5$  at POPG/wsCyt  $b_5$  molar ratio of 25:1 and (d) in the absence of protein. Solid line, first heating; broken line, second heating.



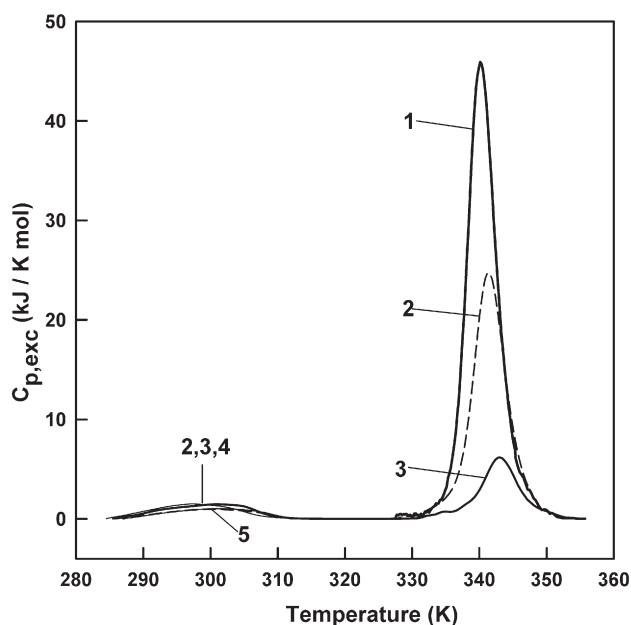


Fig. 3. Excess partial heat capacity,  $C_{p,exc}$  as a function of temperature for wsCyt  $b_5$  at pH 7.2 in the presence of vesicles from mixed (1:1) phospholipids of uncharged saturated DPPC and negatively charged unsaturated POPG at total (DPPC/POPG)/wsCyt  $b_5$  molar ratios of 25:1 (2), 50:1 (3) and 100:1 (4). Heat absorption curve for wsCyt  $b_5$  in the native state, pH 7.2, (1) and that for pure DPPC vesicles (curve 5) are shown for comparison.  $C_{p,exc}$  peak in the range of 340 K range was calculated for a protein concentration 0.8 mg/ml and the  $C_{p,exc}$  peak in the range of 315 K was calculated for the appropriate concentration of DPPC.

the temperature range is observed for pure vesicles, which may indicate simple binding of the protein to the membrane surface. Dramatic changes in the temperature range for melting of pure vesicles at pH 5.5 may reflect protein-vesicle interactions and phospholipid packing and/or vesicle-vesicle interactions in the presence of the denatured protein, as well as the penetration of the protein into membrane bilayer. Interestingly, reducing the negative charge at the membrane surface by half (POPG:DPPC/1:1 phospholipids) while maintaining constant total lipid concentration results in a similar qualitative result and enhanced thermodynamic effects as evaluated by microcalorimetry. Comparison of the results obtained with POPG vesicles (Fig. 2) with those obtained for POPG/DPPC (1:1) vesicles (Fig. 3) demonstrates that the behavior observed at 25:1 and 50:1 (Fig. 3, curves 2 and 3) L/P for the mixed vesicles is comparable to that observed at 50:1 and 100:1 for the POPG vesicles (Fig. 2, curves 2 and 3) at pH 7.2.

This result is not completely unexpected because wsCyt  $b_5$  functions near the endoplasmic reticulum membrane, which is more neutral than the mitochondrial membrane. Thus, the wsCyt  $b_5$  heme-binding domain structure may be influenced by less negative membrane surface on the more neutral regions of its molecular surface as opposed to the negatively charged region of the surface surrounding the edge of the heme where it is exposed to solvent [54]. It should be stressed that negative charges are distributed asymmetrically on the protein surface in the region where the heme edge is partially exposed to solvent [54].

### 3.1.2. Size exclusion chromatography

From the microcalorimetric analysis, it is clear that wsCyt  $b_5$  binds to phospholipid vesicles. Gel-chromatography provides an alternative means of detecting the binding of the wsCyt  $b_5$  to vesicles. The results of such experiments for wsCyt  $b_5$  in the presence of POPG vesicles at 7.2 and pH 5.5 at different molar ratio (in the presence of 150 mM NaCl) are shown in Fig. 4. At pH 7.2 and a moderate L/P (50:1 or 200:1, curves 1 and 2, respectively), the retention time exhibited by the wsCyt  $b_5$  is characteristic of that for the native protein while at a higher ratio (500:1, curve 3), the protein elutes together with the vesicles, reflecting the binding of the protein to the membrane surface. At pH 5.5, a similar effect is achieved at a lower phospholipid/protein ratio, i.e. at a 100:1 ratio (curve 4), virtually all of the protein is bound to vesicles.

At a 500:1 L/P, wsCyt  $b_5$  is completely bound to vesicles as demonstrated by the FPLC experiments (Fig. 4). The complete set of data for these conditions is provided. Free, unbound wsCyt  $b_5$  can be obtained only using gel-filtration chromatography. As shown in Fig. 4, no wsCyt  $b_5$  species other than unbound native wsCyt  $b_5$  and wsCyt  $b_5$  bound to vesicles is observed. Thus, upon removal of a denaturing agent (in our case the charged vesicle surface), unbound wsCyt  $b_5$  returns to its native form.

### 3.1.3. UV CD spectroscopy

As is well known, the near-UV CD spectrum of a protein reflects the rigid packing of its amino acid side chains and, thus the tertiary structure of the protein. Consequently, changes to or elimination of spectroscopic features in this region of the spectrum indicate changes in or loss of tertiary structure. The near-UV CD spectra of wsCyt  $b_5$  at pH 5.5 and 7.2 in the absence

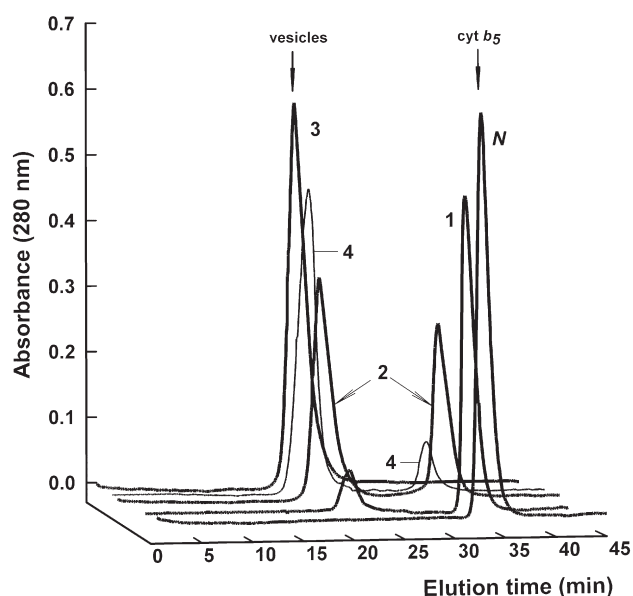


Fig. 4. Elution profiles of wsCyt  $b_5$  in the presence of negatively charged phospholipid vesicles recorded at 280 nm at pH 7.2 for the molar ratio of POPG/wsCyt  $b_5$  50:1 (1), 200:1 (2) and 500:1 (3). The elution profile observed at pH 5.5 at 100:1 (4) and 200:1, which coincides with elution profile of 500:1 at pH 7.2 (3). N – the elution profile of wsCyt  $b_5$  in the absence of vesicles. Arrows indicate the elution time of pure vesicles and wsCyt  $b_5$  markers.

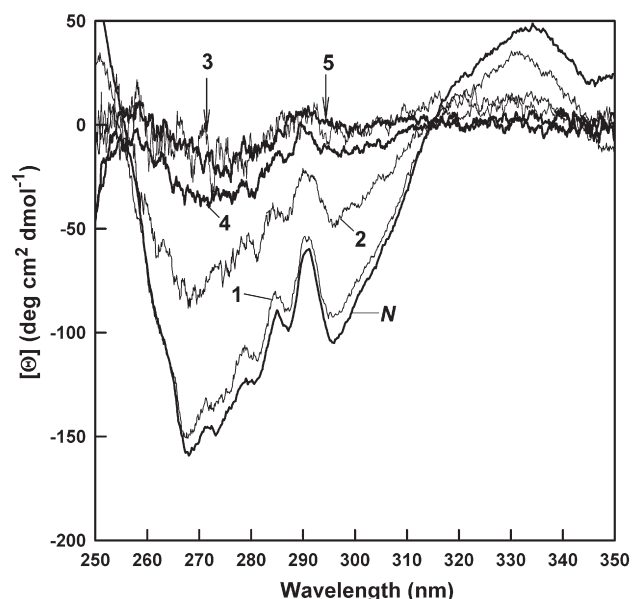


Fig. 5. Near-UV CD spectra of wsCyt  $b_5$  in the absence (N, it is the same for both pH 7.2 and pH 5.5) and in the presence of negatively charged phospholipid vesicles at pH 7.2 and POPG/wsCyt  $b_5$  molar ratios of 50:1 (1), 200:1 (2), and 500:1 (3) and at pH 5.5 for POPG/wsCyt  $b_5$  molar ratios of 50:1 (4) and 100:1 (5).

and in the presence of POPG vesicles are shown in Fig. 5. The spectrum of wsCyt  $b_5$  in the absence of vesicles at pH 7.2 has a unique shape with a number of features apparent (Fig. 5, curve N). The ellipticity observed for wsCyt  $b_5$  in the presence of vesicles is reduced significantly with increasing phospholipid concentration. At pH 7.2 (Fig. 5), the protein structure is affected by the presence of negatively charged vesicles only at high L/P – 200:1 and 500:1 (curves 2 and 3), while at pH 5.5, a similar effect is observed at an L/P ratio of just 50:1 (curve 4). This loss of ellipticity in this region of the spectrum is consistent with relaxation in side-chain packing and the loss of tertiary structure. To evaluate the character of this structural rearrangement further, additional spectroscopic studies were performed.

The observation of the heat absorption peak for wsCyt  $b_5$  at pH 5.5 provides evidence for the presence of a rigid tertiary structure under these conditions, and the near-UV CD spectrum at pH 5.5 is identical to that observed at pH 7.2 (Fig. 5, N), but stability of this structure is reduced.

#### 3.1.4. Electronic absorption spectroscopy

The electronic spectra of wsCyt  $b_5$  in the presence of POPG vesicles at various L/P (pH 7.2 and 5.5) are compared with the corresponding spectra of the native (N) and molten-globule (MG) forms of the protein in Fig. 6. Both the line shape and intensity of these spectra vary with conditions. At pH 7.2 (Fig. 6), gradual changes are observed with increasing L/P such that the Soret band broadens and shifts to shorter wavelengths (see curves 1–3). In addition, a shoulder appears around 370–380 nm as expected with protein denaturation. However, the absorbance spectrum even at L/P of 500:1 (curve 3) is distinct from the spectrum of the molten-globule form at pH 3. Thus, with increasing L/P (pH 7.2), the heme environment becomes increasingly non-native, but heme is still bound to the protein

(the unbound heme in the presence of vesicles exhibits a rather broad absorbance maximum in the 300–400 nm range) because in the MG state at pH 3.0 heme dissociated from the wsCyt  $b_5$ . Even if heme had been dissociated completely from the protein, its hydrophobic nature would result in its accumulation in the lipid bilayer. In any case, heme is not released into aqueous solution because no precipitant was observed as would be expected at pH 3.0. Notably, increasing ionic strength in the presence of vesicles restores the Soret band (data not shown), consistent with the release of the protein from the vesicles and restoration of the heme native environment. Thus, we suggest that at pH 7.2 the dominant stabilizing interactions between wsCyt  $b_5$  and vesicles are electrostatic.

At pH 5.5 (Fig. 6, inset), even a 50:1 L/P ratio induces a dramatic change in the Soret spectrum (curve 1), and increasing this ratio further results in little additional change (curves 2 and 3). Specifically, addition of phospholipid vesicles at pH 5.5 broadens and shifts the Soret maximum to 400 nm relative to the spectrum of the native protein while the intensity remains relatively high. These changes reflect profound changes in the heme environment and substantial protein denaturation. The relatively high absorbance intensity observed at this pH may reflect greater proximity of the heme to the hydrophobic region of the bilayer. Again, the shoulder at 370 nm indicates changes in the heme environment related to protein denaturation, which is substantially greater at pH 5.5. The electronic spectrum of hemin in the presence of vesicles but without protein (pH 5.5) also exhibits greater intensity relative to that of hemin in buffer alone but the maximum absorbance occurs at ~380 nm (data not shown).

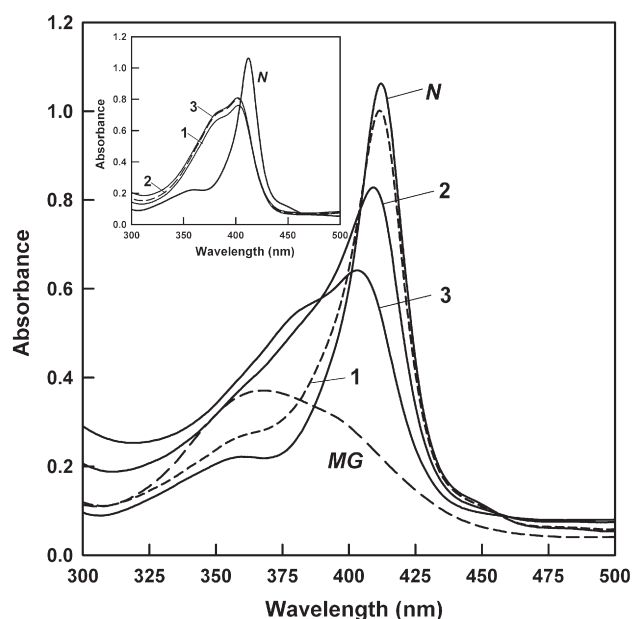


Fig. 6. Absorbance spectra of wsCyt  $b_5$  in the presence of negatively charged phospholipid vesicles at pH 7.2 and POPG/wsCyt  $b_5$  molar ratios of 50:1 (1), 200:1 (2), 500:1 (3) and (Inset) at pH 5.5 and POPG/wsCyt  $b_5$  molar ratios of 50:1 (1), 100:1 (2) and 200:1 (3). Absorbance spectra of native (N) wsCyt  $b_5$  without vesicles at both pH values and the molten-globule (MG) at pH 3.0 are shown for comparison.

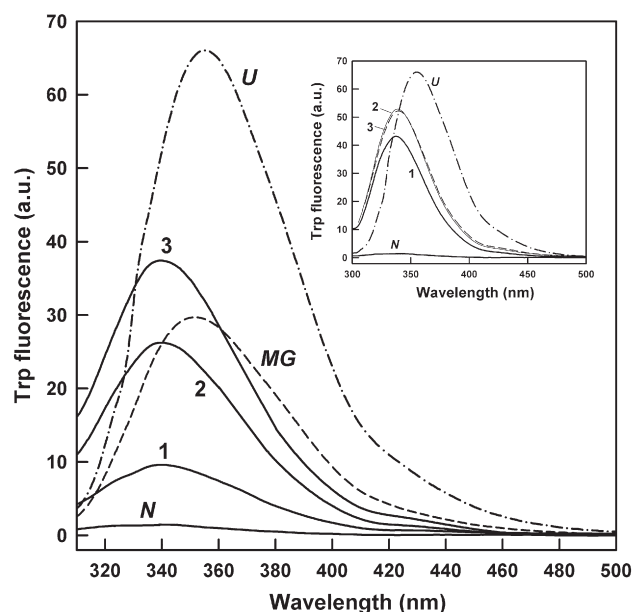


Fig. 7. Changes in tryptophan fluorescence of wsCyt  $b_5$  in the presence of negatively charged phospholipid vesicles at pH 7.2 and POPG/wsCyt  $b_5$  molar ratios of 50:1 (1), 200:1 (2), and 500:1 (3) and (Inset) at pH 5.5, at POPG/wsCyt  $b_5$  molar ratios of 50:1 (1), 100:1 (2) and 200:1 (3). For comparison, the spectra for the wsCyt  $b_5$  without vesicles at both pH (N) and for the unfolded protein (U, 6.0 M GdmCl) are also shown, and that for the MG state at pH 3.0 is shown in the figure.

### 3.1.5. Tryptophan fluorescence emission spectroscopy

The heme-binding domain of cytochrome  $b_5$  possesses one Trp residue that is located in the  $\beta$ -sheet region of the protein molecule [54], while the region of the domain that binds heme non-covalently is helical in nature. In the native protein, Trp fluorescence is strongly quenched by its proximity to the heme and other specific residues (e.g., Met, Lys, Leu) [55,56]. The change in wsCyt  $b_5$  Trp fluorescence that results from exposure to vesicles at various L/P and that occurs in various conformational states (N; U, MG only in Fig. 7) are presented in Fig. 7. At pH 7.2 (Fig. 7, curves 1–3), the intensity of Trp fluorescence gradually increases but the position of the absorption maxima remains approximately the same as in the native protein. Both the wavelength of maximum Trp fluorescence emission and the emission intensity that occur with addition of vesicles are quite different from that of unfolded state. At pH 5.5 (Fig. 7, inset, curves 1–3) the increased intensity of Trp emission is even greater than observed at pH 7.2, but as before, the emission wavelength maximum does not change. The increased Trp fluorescence intensity observed presumably arises from the increasing distance between the Trp and its quenchers and changes in their mutual orientation, i.e. protein denaturation but not complete unfolding. As suggested above, the changes in emission spectrum observed in these experiments may be explained by the compactness of the protein and a more hydrophobic environment for the Trp residue that results from proximity to the hydrophobic region of the bilayer [56] and, probably, to more intimate interaction of the protein with vesicles, especially at pH 5.5.

Native wsCyt  $b_5$  (unbound) does not exhibit fluorescence emission by the one Trp residue, which it possesses, owing to efficient quenching by the heme. Thus, increasing Trp fluorescence intensity in the presence of charged vesicles reflects only the behavior of bound wsCyt  $b_5$  or unbound protein with strongly destabilized tertiary structure in Trp environment. In either case, increased Trp fluorescence is observed here only in the presence of a lipid interface.

### 3.2. Secondary structure (far-UV CD spectroscopy)

The influence of phospholipid vesicles on far-UV CD spectra of wsCyt  $b_5$  was evaluated at pH 7.2 and 5.5 (Fig. 8). Changes occur mainly at 220 nm and indicate primarily changes in  $\alpha$ -helical content, because changes in  $\beta$ -structure are not

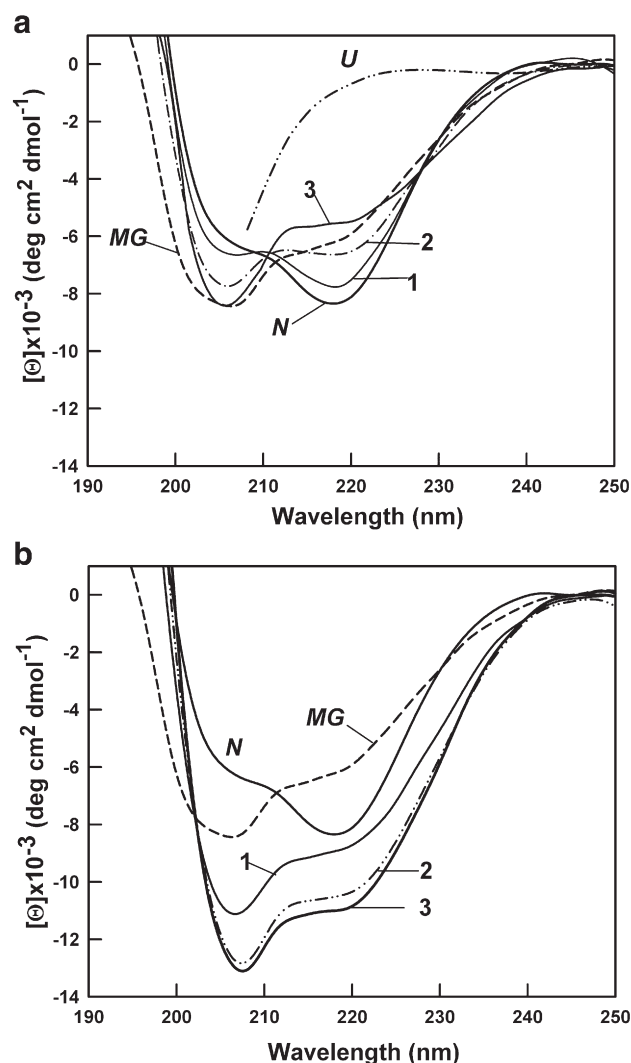


Fig. 8. Far-UV CD spectra of wsCyt  $b_5$  in the presence of negatively charged phospholipid vesicles at (a) pH 7.2 and POPG/wsCyt  $b_5$  molar ratios of 50:1 (1), 200:1 (2) and 500:1 (3) and (b) pH 5.5 and POPG/wsCyt  $b_5$  molar ratios of 50:1 (1), 100:1 (2) and 200:1 (3). For comparison, the spectra for the native protein (N) without vesicles at both pH and the molten-globule state (MG, pH 3.0) are also shown. The spectrum of the unfolded protein (U, 6.0 M GdmCl) is shown only in panel (a).

observed clearly in this part of the spectrum. As seen in this figure, the far-UV CD spectra are distinct and well-structured at both values of pH in the presence of negatively charged (POPG) vesicles. However, at pH 7.2 (Fig. 8 a, curves 1–3) increasing L/P induces changes in the line shape of the spectrum that are characteristic of the transition from the native to the molten globule-like intermediate. Under all conditions examined at this pH in the absence of denaturant (except unfolded state U), the presence of pronounced secondary structure in the protein is readily apparent.

At pH 5.5 (Fig. 8 b, curves 1–3), addition of vesicles increases the negative ellipticity evident in the spectra and induces line shape changes, even at the lowest L/P, that are typical of the molten-globule state of many proteins. Increased negative ellipticity at 220 nm indicates an increase in secondary structure content. Similar changes in the far-UV CD spectra of wsCyt  $b_5$  are observed in the presence of high concentrations of alcohol (methanol [16] and methanol and isopropanol (unpublished data)). Such an effect can be explained by preferential binding of

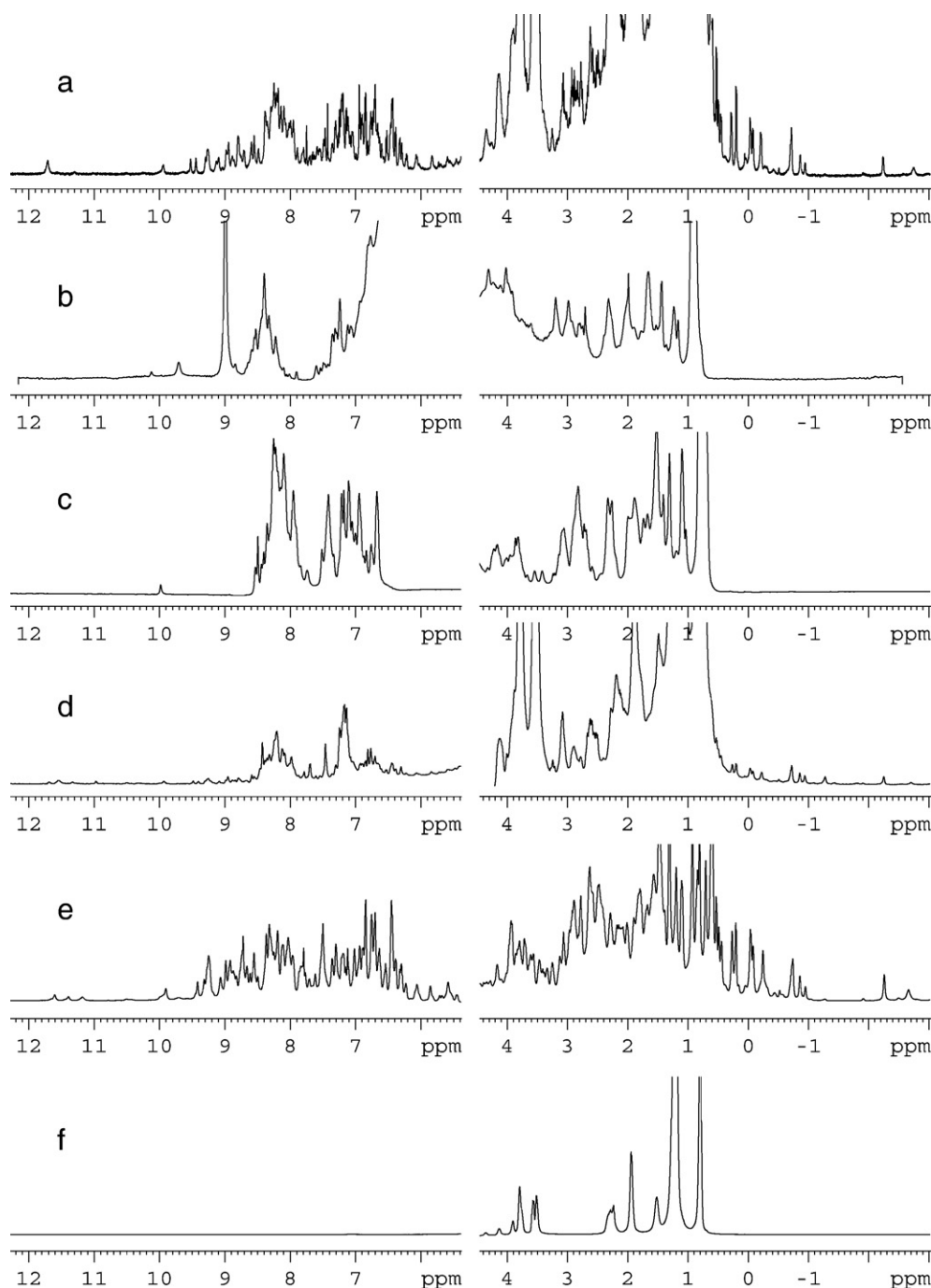


Fig. 9.  $^1\text{H}$ -NMR spectra of wsCyt  $b_5$ : (a) the protein in the presence of negatively charged phospholipids vesicles at POPG/wsCyt  $b_5$  50:1, pH 7.2; (b) the unfolded protein in 9 M urea, pH 7.2 without vesicles; (c) the protein in the molten-globule state at pH 3.0 in the absence of vesicles; (d) the protein in the presence of vesicles at POPG/wsCyt  $b_5$  50:1, pH 5.5; (e) the native protein, pH 5.5, without vesicles; (f) POPG vesicles without protein, pH 7.2, shown in reduced scale.



organic solvent to  $\alpha$ -helical structures, i.e. enhancing the stability of hydrogen bonding within the polypeptide chain. Thus, we suggest that the increased intensity observed at 220 nm at pH 5.5 may be explained by increased protein-membrane interaction that may even involve insertion of a part of the wsCyt  $b_5$  structure into the phospholipid bilayer. The results reported above suggest further that the loss of tertiary structure does not lead to a decrease or loss of secondary structure.

### 3.3. $^1\text{H-NMR}$ Spectroscopy

To initiate more detailed spectroscopic characterization of the structural changes in wsCyt  $b_5$  that are induced by interaction with phospholipids membranes,  $^1\text{H-NMR}$  spectra of wsCyt  $b_5$  (Fig. 9) in the native state at pH 5.5 (Fig. 9 e) and of wsCyt  $b_5$  in the presence of vesicles have been obtained at L/P of 50:1 and pH 7.2 (Fig. 9 a). Control spectra of pure POPG vesicles (Fig. 9 f) and denatured wsCyt  $b_5$  in 9 M urea (Fig. 9 b) are also shown. As can be seen, the native protein as well as wsCyt  $b_5$  in the presence of vesicles (L/P of 50:1 and pH 7.2) exhibit specific chemical shift dispersion for aromatic groups, for heme signals in the 12–6 ppm region and for high field resonances in 1–(–3) ppm region (Fig. 9 a, e) whereas the main resonances of pure POPG vesicles occur at 4–1 ppm (Fig. 9 f). At L/P of 50:1 and pH 5.5, resonances in the aromatic region (Fig. 9 d) change, the number of high field resonances decreases significantly, and this region of the  $^1\text{H-NMR}$  spectrum becomes similar to that of the molten-globule intermediate form observed in the absence of vesicles at pH 3.0 (Fig. 9 c). NMR evidence for induction of the wsCyt  $b_5$  molten-globule form has not been reported previously.

## 4. Discussion

Our results establish that the water-soluble heme-binding domain of cytochrome  $b_5$  loses its rigid tertiary structure in the presence of negatively charged vesicles while retaining a distinct secondary structure and reasonable compactness. Furthermore, our results indicate that the relaxed form of the protein interacts with and binds to the artificial model membrane structure. This conclusion is consistent with our hypothesis that a membrane surface with negatively charged phospholipids can act as a mild denaturing agent in the cytoplasm and can induce formation of non-native protein conformational states in a negatively charged protein.

While the influence of a negatively charged membrane surface on the structure of a negatively charged protein can be demonstrated in studies of this type in vitro, corresponding studies under conditions that simulate the conditions that are relevant in vivo are extremely difficult to design, perform and interpret because the conditions are (a) not amenable to the experimental methods available and (b) far from ideality. Cytoplasm can be regarded as a sol-gel with total concentration of macromolecules of  $\sim 350$  mg/mL [57] and with up to 50% of cellular protein in the solid phase [58]. Under these conditions, the activity of water is much different from that of dilute aqueous solution, and the electrostatic contributions of charged groups of

proteins are difficult to model and to quantify. Thus, although the choice and concentrations of phospholipids used in this study are not identical to those present in the relevant biological membranes, it is unlikely that phospholipids of varying chemical identity differ significantly in their electrostatic properties for the purpose of this study. In view of these other, more significant, environmental factors that are rarely if ever taken into account in studies of this type, rigorous simulation of conditions that operate in vivo is difficult if not impossible without development of new experimental techniques that are compatible with such extreme requirements.

It should be emphasized once more that negatively charged residues of wsCyt  $b_5$  are located mainly near the heme edge and the remaining surface of wsCyt  $b_5$  has a net charge of (–1). Thus, in principle, its structure may be influenced by negatively charged surface of vesicles upon their collisions as for other proteins. Our observation that wsCyt  $b_5$  can exhibit structural flexibility consistent with formation of a molten globule-like state in the presence of artificial membranes may be relevant to several functional properties of this protein that have been reported previously. For example, the mechanism of cytochrome  $b_5$  heme-binding orientation equilibration characterized in detail by La Mar and colleagues [59–62] may involve formation of relaxed conformational intermediates similar to those identified here. Specifically, the initial complex formed on addition of heme to apo-cytochrome  $b_5$  is a mixture of equal proportions of complexes that differ only by rotation of the heme by  $180^\circ$  around the  $\alpha$ - $\gamma$  meso-carbon axis. After a few minutes, equilibrium is established and 90% of the ferricytochrome exhibits one of the two-heme binding orientations. This equilibration process could reasonably be expected to involve transient conformational intermediates of the type observed in the present study.

On the other hand, the transfer of heme from ferricytochrome  $b_5$  to apomyoglobin [63], which may occur in the endoplasmic reticulum (ER) membrane field or close to the junction between the ER and mitochondria, presumably requires relaxation of the structures of both proteins. Similarly, a relaxed tertiary structure would facilitate the acquisition of heme by apo-wsCyt  $b_5$  when it binds near the mitochondrial membrane or during transfer of heme from putative heme-binding (or transferring) proteins.

Conformational changes and interaction of positively charged proteins with artificial membranes are well studied. They include cytochromes type  $c$  [3, 8–11], fatty acid-binding proteins [64,65], toxins [66–68], acetylcholinesterase [69],  $\alpha$ -lactalbumin [70], and others. These studies show that these proteins acquire a partly folded state upon interaction with membranes. The present work reveals that even wsCyt  $b_5$ , a highly negatively charged protein, is able to change its conformation in the presence of anionic lipid membranes, and these changes may be physiologically important.

The present studies employ artificial model systems with very simple surfaces that lack many components of true cellular membranes. As a result, our findings demonstrate trends in conformational change that a protein structure can undergo in the presence of membrane surfaces and establish the possibility of structural changes that can influence the functional properties of the protein. Related effects have been reported from a much different

experimental approach by Rivas et al. [71] who have observed electrochemical and spectroscopic changes in the properties of cytochrome  $c_3$  located in proximity to self-assembled monolayers formed on an electrode surface. Notably, our observation that the tertiary structure of wsCyt  $b_5$  can be affected in the presence of a charged membrane surface may have implications for electron-transfer between wsCyt  $b_5$  and its partners. In particular, the expectation that the exclusion or reduction of the amount of water present at the interface of two electron-transfer proteins in proximity to the heme edge [72–77] could have structural consequences at least in part related to those described in the current experiments that could influence electron-transfer kinetics. Clearly, this hypothetical/theoretical possibility merits further experimental investigation. However, it should be noted that the entropic stabilization of cytochrome  $b_5$ –cytochrome  $c$  complex formation as the result of complex formation-induced solvent displacement was first demonstrated by titrations based on electronic difference spectroscopy over 25 years ago [74] and subsequently confirmed by isothermal titration calorimetry [75].

In summary, the current studies demonstrate the remarkable finding that in the presence of vesicles (L/P=50:1) under conditions that a substantial amount of wsCyt  $b_5$  remains unbound (Fig. 4, curve 1), the tertiary structure of the protein is significantly destabilized by the presence of anionic membranes. Specifically, while the melting temperature  $T_d$  practically remains unchanged, the  $C_{p,exc}$  maximum decreases considerably (compare Fig. 1, curve 1, and Fig. 2a, curve 2) under such conditions. These observations may have more general implications for structural consequences at the surfaces of protein-protein electron-transfer complexes involving cytochrome  $b_5$  and its partners in which at least partial solvent exclusion may occur prior to electron-transfer.

## Acknowledgements

We are grateful to D.A. Prokhorov for the assistance with the NMR experiments and discussion of the results. This work was supported partly by INTAS (grant 01-2126), HHMI (awards 55000305 and 55005607 to A.V. Finkelstein), the Russian Foundation for Basic Research (grant 02-04-48748), RAS Programs “Molecular and Cellular Biology” and “Scientific Schools” #1968.2003.4, CIHR grant MOP-7182 (AGM) and a Canada Research Chair (AGM).

## References

- [1] O.B. Ptitsyn, Molten globule and protein folding, *Adv. Protein Chem.* 47 (1995) 83–229.
- [2] V.E. Bychkova, O.B. Ptitsyn, The molten globule *in vitro* and *in vivo*, *Chemtracts: Biochem. Mol. Biol.* 4 (1993) 133–163.
- [3] V.E. Bychkova, A.E. Dujsekina, S.I. Klenin, E.I. Tiktopulo, V.N. Uversky, O.B. Ptitsyn, Molten globule-like state of cytochrome  $c$  under conditions simulating those near the membrane surface, *Biochemistry* 35 (1996) 6058–6063.
- [4] K.D. Wilkinson, A.N. Mayer, Alcohol-induced conformational changes of ubiquitin, *Arch. Biochem. Biophys.* 250 (1986) 390–399.
- [5] E. Dufour, C. Bertrand-Harb, T. Haertle, Reversible effects of medium dielectric constant on structural transformation of beta-lactoglobulin and its retinol binding, *Biopolymers* 33 (1993) 589–598.
- [6] V.E. Bychkova, A.E. Dujsekina, A. Fantuzzi, O.B. Ptitsyn, G.L. Rossi, Release of retinol and denaturation of its plasma carrier, retinol-binding protein, *Fold. Des.* 3 (1998) 285–291.
- [7] V.E. Bychkova, R. Berni, G.L. Rossi, V.P. Kutysenko, O.B. Ptitsyn, Retinol-binding protein is in the molten globule state at low pH, *Biochemistry* 31 (1992) 7566–7571.
- [8] H.H. de Jongh, J.A. Killian, B. de Kruijff, A water-lipid interface induces a highly dynamic folded state in apocytochrome  $c$  and cytochrome  $c$ , which may represent a common folding intermediate, *Biochemistry* 31 (1992) 1636–1643.
- [9] T.J. Pinheiro, G.A. Elove, A. Watts, H. Roder, Structural and kinetic description of cytochrome  $c$  unfolding induced by the interaction with lipid vesicles, *Biochemistry* 36 (1997) 13122–13132.
- [10] S. Ollerich, S. Lecocmte, M. Paternostre, T. Heimburg, P. Hildebrandt, Peripheral and integral binding of cytochrome  $c$  to phospholipid vesicles, *J. Phys. Chem. B* 108 (2004) 3871–3878.
- [11] S. Bernad, S. Oellerich, T. Soulimane, S. Noinville, M.H. Baron, M. Paternostre, S. Lecomte, Interaction of horse heart and *Thermus thermophilus* type  $c$  cytochromes with phospholipid vesicles and hydrophobic surfaces, *Biophys. J.* 86 (2004) 3863–3872.
- [12] Y.O. Kamatari, S. Ohji, T. Konno, Y. Seki, K. Soda, M. Kataoka, K. Akasaka, The compact and expanded denatured conformations of apomyoglobin in the methanol-water solvent, *Protein Sci.* 8 (1999) 873–882.
- [13] L.V. Basova, E.I. Tiktopulo, I.A. Kashparov, V.E. Bychkova, Conformational status of apomyoglobin in the presence of phospholipid vesicles at neutral pH, *Mol. Biol. (Mosk)* 38 (2004) 323–332.
- [14] K.R. Babu, D.J. Douglas, Methanol-induced conformations of myoglobin at pH 4.0, *Biochemistry* 39 (2000) 14702–14710.
- [15] L.V. Basova, E.I. Tiktopulo, V.E. Bychkova, Model phospholipid membranes affect the holomyoglobin structure: conformational changes at pH 6.2, *Mol. Biol. (Mosk)* 39 (2005) 120–128.
- [16] Z.Q. Wang, Y.H. Wang, W. Qian, H.H. Wang, L.J. Chunyu, Y. Xie, Z.X. Huang, Methanol-induced unfolding and refolding of cytochrome  $b_5$  and its P40V mutant monitored by UV-visible, CD, and fluorescence spectra, *J. Protein Chem.* 18 (1999) 547–555.
- [17] L. Spatz, P. Strittmatter, A form of cytochrome  $b_5$  that contains an additional hydrophobic sequence of 40 amino acid residues, *Proc. Natl. Acad. Sci. USA* 68 (1971) 1042–1046.
- [18] P. Strittmatter, J. Ozols, The restricted tryptic cleavage of cytochrome  $b_5$ , *J. Biol. Chem.* 241 (1966) 4787–4792.
- [19] L.S. Reid, A.G. Mauk, Kinetics analysis of cytochrome  $b_5$  reduction by  $\text{FeEDTA}^{2-}$ , *J. Am. Chem. Soc.* 104 (1982) 841–845.
- [20] F.S. Mathews, The structure, function and evolution of cytochromes, *Prog. Biophys. Mol. Biol.* 45 (1985) 1–56.
- [21] R.M. Keller, K. Wuthrich, Structural study of the heme crevice in cytochrome  $b_5$  based on individual assignments of the  $^1\text{H}$ -NMR lines of the heme group and selected amino acid residues, *Biochim. Biophys. Acta* 621 (1980) 204–217.
- [22] N.C. Veitch, D.W. Concar, R.J. Williams, D. Whitford, Investigation of the solution structures and mobility of oxidised and reduced cytochrome  $b_5$  by 2D NMR spectroscopy, *FEBS Lett.* 238 (1988) 49–55.
- [23] D. Whitford, The identification of cation-binding domains on the surface of microsomal cytochrome  $b_5$  using  $^1\text{H}$ -NMR paramagnetic difference spectroscopy, *Eur. J. Biochem.* 203 (1992) 211–223.
- [24] R.D. Guiles, J. Altman, I.D. Kuntz, L. Waskell, J.J. Lipka, Structural studies of cytochrome  $b_5$ : complete sequence-specific resonance assignments for the trypsin-solubilized microsomal ferrocytochrome  $b_5$  obtained from pig and calf, *Biochemistry* 29 (1990) 1276–1289.
- [25] F. Lederer, The cytochrome  $b_5$ -fold: an adaptable module, *Biochimie* 76 (1994) 674–692.
- [26] M.R. Mauk, A.G. Mauk, Interaction between cytochrome  $b_5$  and human methemoglobin, *Biochemistry* 21 (1982) 4730–4734.
- [27] M.R. Mauk, A.G. Mauk, P.C. Weber, J.B. Matthew, Electrostatic analysis of the interaction of cytochrome  $c$  with native and dimethyl ester heme substituted cytochrome  $b_5$ , *Biochemistry* 25 (1986) 7085–7091.
- [28] M.R. Mauk, P.D. Barker, A.G. Mauk, Proton linkage of complex formation between cytochrome  $c$  and cytochrome  $b_5$ : electrostatic consequences of protein-protein interactions, *Biochemistry* 30 (1991) 9873–9881.

- [29] A.G. Mauk, M.R. Mauk, G.R. Moore, S.H. Northrup, Experimental and theoretical analysis of the interaction between cytochrome *c* and cytochrome *b<sub>5</sub>*, *J. Bioenerg. Biomembr.* 27 (1995) 311–330.
- [30] K.K. Rodgers, S.G. Sligar, Mapping electrostatic interactions in macromolecular associations, *J. Mol. Biol.* 221 (1991) 1453–1460.
- [31] J.B. Schenkman, I. Jansson, The many roles of cytochrome *b<sub>5</sub>*, *Pharmacol. Ther.* 97 (2003) 139–152.
- [32] F.S. Mathews, M. Levine, P. Argos, Three-dimensional Fourier synthesis of calf liver cytochrome *b<sub>5</sub>* at 2–8 Å resolution, *J. Mol. Biol.* 64 (1972) 449–464.
- [33] J. Mitoma, A. Ito, The carboxy-terminal 10 amino acid residues of cytochrome *b<sub>5</sub>* are necessary for its targeting to the endoplasmic reticulum, *EMBO J.* 11 (1992) 4197–4203.
- [34] F. Kuma, R.A. Prough, B.S. Masters, Studies on methemoglobin reductase. Immunochemical similarity of soluble methemoglobin reductase and cytochrome *b<sub>5</sub>* of human erythrocytes with NADH-cytochrome *b<sub>5</sub>* reductase and cytochrome *b<sub>5</sub>* of rat liver microsomes, *Arch. Biochem. Biophys.* 172 (1976) 600–607.
- [35] R. Goto-Tamura, Y. Takesue, S. Takesue, Immunological similarity between NADH-cytochrome *b<sub>5</sub>* reductase of erythrocytes and liver microsomes, *Biochim. Biophys. Acta* 423 (1976) 293–302.
- [36] D.E. Hultquist, L.J. Sannes, D.A. Schafer, The NADH/NADPH-methemoglobin reduction system of erythrocytes, *Prog. Clin. Biol. Res.* 55 (1981) 291–309.
- [37] K. Fukushima, A. Ito, T. Omura, R. Sato, Occurrence of different types of cytochrome *b<sub>5</sub>*-like hemoprotein in liver mitochondria and their intramitochondrial localization, *J. Biochem. (Tokyo)* 71 (1972) 447–461.
- [38] M. Rivera, C. Barillas-Mury, K.A. Christensen, J.W. Little, M.A. Wells, F.A. Walker, Gene synthesis, bacterial expression, and <sup>1</sup>H NMR spectroscopic studies of the rat outer mitochondrial membrane cytochrome *b<sub>5</sub>*, *Biochemistry* 31 (1992) 12233–12240.
- [39] T.E. Meyer, M. Rivera, F.A. Walker, M.R. Mauk, A.G. Mauk, M.A. Cusanovich, G. Tollin, Laser flash photolysis studies of electron-transfer to the cytochrome *b<sub>5</sub>*-cytochrome *c* complex, *Biochemistry* 32 (1993) 622–627.
- [40] S. Silchenko, M.L. Sippel, O. Kuchment, D.R. Benson, A.G. Mauk, A. Altuve, M. Rivera, Hemin is kinetically trapped in cytochrome *b<sub>5</sub>* from rat outer mitochondrial membrane, *Biochem. Biophys. Res. Commun.* 273 (2000) 467–472.
- [41] A. Altuve, S. Silchenko, K.H. Lee, K. Kuczera, S. Terzyan, X. Zhang, D.R. Benson, M. Rivera, Probing the differences between rat liver outer mitochondrial membrane cytochrome *b<sub>5</sub>* and microsomal cytochromes *b<sub>5</sub>*, *Biochemistry* 40 (2001) 9469–9483.
- [42] V.V. Reddy, D. Kupfer, E. Caspi, Mechanism of C-5 double bond introduction in the biosynthesis of cholesterol by rat liver microsomes, *J. Biol. Chem.* 252 (1977) 2797–2801.
- [43] P. Strittmatter, L. Spatz, D. Corcoran, M.J. Rogers, B. Setlow, R. Redline, Purification and properties of rat liver microsomal stearyl coenzyme A desaturase, *Proc. Natl. Acad. Sci. U. S. A.* 71 (1974) 4565–4569.
- [44] D.J. Livingston, S.J. McLachlan, G.N. La Mar, W.D. Brown, Myoglobin: cytochrome *b<sub>5</sub>* interactions and the kinetic mechanism of metmyoglobin reductase, *J. Biol. Chem.* 260 (1985) 15699–15707.
- [45] P. Strittmatter, J.M. Kittler, J.E. Coghill, J. Ozols, Characterization of lysyl residues of NADH-cytochrome *b<sub>5</sub>* reductase implicated in charge-pairing with active-site carboxyl residues of cytochrome *b<sub>5</sub>* by site-directed mutagenesis of an expression vector for the flavoprotein, *J. Biol. Chem.* 267 (1992) 2519–2523.
- [46] H. Yamazaki, W.W. Johnson, Y.F. Ueng, T. Shimada, F.P. Guengerich, Lack of electron transfer from cytochrome *b<sub>5</sub>* in stimulation of catalytic activities of cytochrome P450 3A4. Characterization of a reconstituted cytochrome P450 3A4/NADPH-cytochrome P450 reductase system and studies with apo-cytochrome *b<sub>5</sub>*, *J. Biol. Chem.* 271 (1996) 27438–27444.
- [47] P.S. Stayton, T.L. Poulos, S.G. Sligar, Putidaredoxin competitively inhibits cytochrome *b<sub>5</sub>*-cytochrome P-450cam association: a proposed molecular model for a cytochrome P-450cam electron-transfer complex, *Biochemistry* 28 (1989) 8201–8205.
- [48] L.V. Basova, N.B. Il'ina, K.S. Vasilenko, E.I. Tiktopulo, V.E. Bychkova, Conformational states of the water-soluble fragment of cytochrome *b<sub>5</sub>*. I. pH-induced denaturation, *Mol. Biol. (Mosk)* 36 (2002) 891–900.
- [49] M. Prats, J. Teissié, J.F. Toccanne, Lateral proton conduction at lipid–water interfaces and its implications for the chemiosmotic-coupling hypothesis, *Nature* 322 (1986) 756–758.
- [50] W.D. Funk, T.P. Lo, M.R. Mauk, G.D. Brayer, R.T. MacGillivray, A.G. Mauk, Mutagenic, electrochemical, and crystallographic investigation of the cytochrome *b<sub>5</sub>* oxidation-reduction equilibrium: Involvement of asparagine-57, serine-64, and heme propionate-7, *Biochemistry* 29 (1990) 5500–5508.
- [51] F. Szoka Jr., D. Papahadjopoulos, Comparative properties and methods of preparation of lipid vesicles (liposomes), *Annu. Rev. Biophys. Bioeng.* 9 (1980) 467–508.
- [52] O.I. Lebed, A.V. Stefanov, R.G. Primak, Effect of the conditions of ultrasonic treatment on the characteristics of forming liposomes, *Ukr. Biokhim. Zh.* 61 (1989) 96–101.
- [53] P.L. Privalov, S.A. Potekhin, Scanning microcalorimetry in studying temperature-induced changes in proteins, *Methods Enzymol.* 131 (1986) 4–51.
- [54] R.C. Durley, F.S. Mathews, Refinement and structural analysis of bovine cytochrome *b<sub>5</sub>* at 1.5 Å resolution, *Acta Crystallogr., D Biol. Crystallogr.* 52 (1996) 65–76.
- [55] Y. Chen, M.D. Barkley, Toward understanding tryptophan fluorescence in proteins, *Biochemistry* 37 (1998) 9976–9982.
- [56] A.S. Ladokhin, S.H. White, Alphas and taus of tryptophan fluorescence in membranes, *Biophys. J.* 81 (2001) 1825–1827.
- [57] S.B. Zimmerman, A.P. Minton, Macromolecular crowding: biochemical, biophysical, and physiological consequences, *Annu. Rev. Biophys. Biomol. Struct.* 22 (1993) 27–65.
- [58] K. Luby-Phelps, Cytoarchitecture and physical properties of cytoplasm: volume, viscosity, diffusion, intracellular surface area, *Int. Rev. Cytol.* 192 (2000) 189–221.
- [59] G.N. La Mar, P.D. Burns, J.T. Jackson, K.M. Smith, K.C. Langry, P. Strittmatter, Proton magnetic resonance determination of the relative heme orientations in disordered native and reconstituted ferricytochrome *b<sub>5</sub>*. Assignment of heme resonances by deuterium labeling, *J. Biol. Chem.* 256 (1981) 6075–6079.
- [60] K.B. Lee, G.N. La Mar, L.A. Kehres, E.M. Fujinari, K.M. Smith, T.C. Pochapsky, S.G. Sligar, <sup>1</sup>H NMR study of the influence of hydrophobic contacts on protein-prosthetic group recognition in bovine and rat ferricytochrome *b<sub>5</sub>*, *Biochemistry* 29 (1990) 9623–9631.
- [61] K.B. Lee, G.N. La Mar, R.K. Pandey, I.N. Rezzano, K.E. Mansfield, K.M. Smith, <sup>1</sup>H NMR study of the role of heme carboxylate side chains in modulating heme pocket structure and the mechanism of reconstitution of cytochrome *b<sub>5</sub>*, *Biochemistry* 30 (1991) 1878–1887.
- [62] S.J. McLachlan, G.N. La Mar, P.D. Burns, K.M. Smith, K.C. Langry, <sup>1</sup>H-NMR assignments and the dynamics of interconversion of the isomeric forms of cytochrome *b<sub>5</sub>* in solution, *Biochim. Biophys. Acta* 874 (1986) 274–284.
- [63] L.L. Xue, Y.H. Wang, Y. Xie, P. Yao, W.H. Wang, W. Qian, Z.X. Huang, J. Wu, Z.X. Xia, Effect of mutation at valine 61 on the three-dimensional structure, stability, and redox potential of cytochrome *b<sub>5</sub>*, *Biochemistry* 38 (1999) 11961–11972.
- [64] V. Nolan, M. Perduca, H.L. Monaco, B. Maggio, G.G. Montich, Interactions of chicken liver basic fatty acid-binding protein with lipid membranes, *Biochim. Biophys. Acta* 1611 (2003) 98–106.
- [65] M.B. Decca, M. Perduca, H.L. Monaco, G.G. Montich, Conformational changes of chicken liver bile acid-binding protein bound to anionic lipid membrane are coupled to the lipid phase transitions, *Biochim. Biophys. Acta* 1768 (2007) 1583–1591.
- [66] C. Guidi-Rontani, M. Weber-Levy, M. Mock, V. Cabiaux, Translocation of *Bacillus anthracis* lethal and oedema factors across endosome membranes, *Cell. Microbiol.* 2 (2000) 259–264.
- [67] C. Lesieur, S. Frutiger, G. Hughes, R. Kellner, F. Pattus, F.G. van der Goot, Increased stability upon heptamerization of the pore-forming toxin aerolysin, *J. Biol. Chem.* 274 (1999) 36722–36728.
- [68] P.J. Day, T.J. Pinheiro, L.M. Roberts, J.M. Lord, Binding of ricin A-chain to negatively charged phospholipid vesicles leads to protein structural changes and destabilizes the lipid bilayer, *Biochemistry* 41 (2002) 2836–2843.

- [69] I. Shin, I. Silman, C. Bon, L. Weiner, Liposome-catalyzed unfolding of acetylcholinesterase from *Bungarus fasciatus*, *Biochemistry* 37 (1998) 4310–4316.
- [70] J. Kim, H. Kim, Interaction of  $\alpha$ -lactalbumin with phospholipid vesicles as studied by photoactivated hydrophobic labeling, *Biochim. Biophys. Acta* 983 (1989) 1–8.
- [71] L. Rivas, C.M. Soares, A.M. Baptista, J. Simaan, R.E. Di Paolo, D.H. Murgida, P. Hildebrandt, Electric-field-induced redox potential shifts of tetraheme cytochromes  $c_3$  immobilized on self-assembled monolayers: surface-enhanced resonance Raman spectroscopy and simulation studies, *Biophys. J.* 88 (2005) 4188–4199.
- [72] F.R. Salemme, An hypothetical structure for an intermolecular electron transfer complex of cytochromes  $c$  and  $b_5$ , *J. Mol. Biol.* 102 (1976) 563–568.
- [73] T.L. Poulos, A.G. Mauk, Models for the complexes formed between cytochrome  $b_5$  and the subunits of methemoglobin, *J. Biol. Chem.* 258 (1983) 7369–7373.
- [74] M.R. Mauk, L.S. Reid, A.G. Mauk, Spectrophotometric analysis of the interaction between cytochrome  $b_5$  and cytochrome  $c$ , *Biochemistry* 21 (1982) 1843–1846.
- [75] M.A. McLean, S.G. Sligar, Thermodynamic characterization of the interaction between cytochrome  $b_5$  and cytochrome  $c$ , *Biochem. Biophys. Res. Commun.* 215 (1995) 316–320.
- [76] J.B. Schenkman, I. Jansson, Interactions between cytochrome P450 and cytochrome  $b_5$ , *Drug Metab. Rev.* 31 (1999) 351–364.
- [77] J. Lin, I.A. Balabin, D.N. Beratan, The nature of aqueous tunneling pathways between electron-transfer proteins, *Science* 310 (2005) 1311–1313.